nature cell biology

Amplitude control of cell-cycle waves by nuclear import

Attila Becskei[1], Monica G. Boselli[2] and Alexander van Oudenaarden[1]

Propagation of waves of biochemical activities through consecutive stages of the cell cycle is essential to execute the steps of cell division in a strict temporal order. Mechanisms that ensure the proper amplitude and timing of these waves are poorly understood[1]. Using a synthetic gene circuit, we show that a transcriptional activator driven by yeast cell-cycle promoters propagates transcriptional oscillations with substantial damping. Although regulated nuclear translocation has been implicated in the timing of oscillatory events[2,3], mathematical analysis shows that increasing the rate of nuclear transport is an example of a general regulatory principle, which enhances the fidelity of wave propagation. Indeed, increasing the constitutive import rate of the activator counteracts the damping of waves and concurrently preserves the intensity of the signal. In contrast to the regulatory range of nuclear transport, the range of mRNA turnover considerably limits transcriptional wave propagation. This classification of cellular processes outlines potential regulatory mechanisms that can contribute to faithful transmission of oscillations at different stages of the cell cycle.

Regulators that function during one stage of the cell cycle trigger events in the next stage[4–6]. If the correct amplitude and timing of the triggered events is altered, progression through the cell cycle is compromised and consequently morphological aberration, genomic instability or cancer may arise[7–9]. To explore the regulation of how a wave of biochemical activity in a cell-cycle stage is propagated into the subsequent stage, we constructed a synthetic gene network using input, transmission and output modules in the yeast *Saccharomyces cerevisiae*. Promoters involved in regulation of cell-cycle progression served as the input modules to drive the expression of a transcriptional activator, rtTA, comprising the VP16 activator and the TetR(S2) DNA binding domains (Fig. 1a). rtTA was chosen to transmit the oscillatory activity of input promoters because it is a transcriptional activator with a broad regulatory range[10]. rtTA in the presence of doxycycline activates the expression of the reporter gene, *lacZ* (β-galactosidase), monitoring the signal propagation process.

The linearity of the transmission was examined by measuring the activity of the output as a function of the input with varying intensities. The activity of β-galactosidase expressed under the direct control of *CLB2*, *CLN2*, *SWI4* and *SWI6* promoters spanned a range of more than two orders of magnitude. The respective output activities show an approximately linear amplification by rtTA in this range (Fig. 1b).

The *CLN2* and *CLB2* promoters were selected for studying the transmission of oscillations because *CLN2* and *CLB2* transcripts display high peak : trough ratios (PTRs; 11 and 14, respectively) and are activated at different stages of the cell cycle (G1 and G2/M, respectively)[11]. The stability of β-galactosidase (half-life greater than 20 h) (ref. 12) precludes it from following rapid changes in the oscillatory input; therefore induction of β-galactosidase by doxycycline was restricted to short periods. To avoid the resulting decrease in β-galactosidase activity, multiple *lacZ* integration was used, which allows for an extended range of amplification[13]. Upon addition of doxycycline, the production of β-galactosidase started after a lag of 15 min (Fig. 1c). A transient induction scheme was designed to restrict transcription of *lacZ* to short periods so that the β-galactosidase activity faithfully reflects the oscillations of the level of nuclear rtTA. This technique illustrates the advantage of having an inducible activator that circumvents the slow response of β-galactosidase (see Supplementary Information). Doxycycline was added at 10 min intervals to a synchronized yeast population, and cells were harvested 30 min after induction to monitor approximately 15 min of *lacZ* expression. The level of nuclear rtTA, driven by the *CLN2* promoter, peaked roughly at the onset of budding (Fig. 1d), whereas the level of rtTA that is driven by the *CLB2* promoter, peaked around 40 min after budding (Fig. 1e). PTR was chosen as a parameter to quantify the strength of oscillations (maximum/minimum value of oscillations). Because it is a relative measure, it allows a comparison of oscillations of different molecular components. Interestingly, in both cases the PTR of nuclear rtTA waves (PTR_{CLN2} = 2.9±0.6 and PTR_{CLB2} = 3.0 ± 0.3) is only about 25% of that reported for the input oscillations. Using higher concentrations of doxycycline shifts the intensity of the output wave to higher values but did not significantly change the PTR (Fig. 1e). These results indicate that cellular processes involved in converting the *rtTA* mRNA to nuclear rtTA protein reduce the PTR of the propagated waves.

The constraints on transmission of oscillations were explored by a mathematical analysis of a sequence of cellular biochemical steps that mediate the transmission of the input signal (see Fig. 2, Methods). The oscillatory input corresponds to the *rtTA* mRNA transcribed from the *CLN2* or *CLB2* promoter, the translation of which results in the first component in the transmission process, the cytoplasmic rtTA.

[1]Department of Physics, Massachusetts Institute of Technology, 13-2008, Cambridge, MA 02139, USA.
[2]Center for Cancer Research, Massachusetts Institute of Technology, E17-233, Cambridge, MA 02139, USA.
Correspondence should be addressed to A.v.O. (e-mail: avano@mit.edu)

Published online: 25 April 2004; DOI: 10.1038/ncb1124

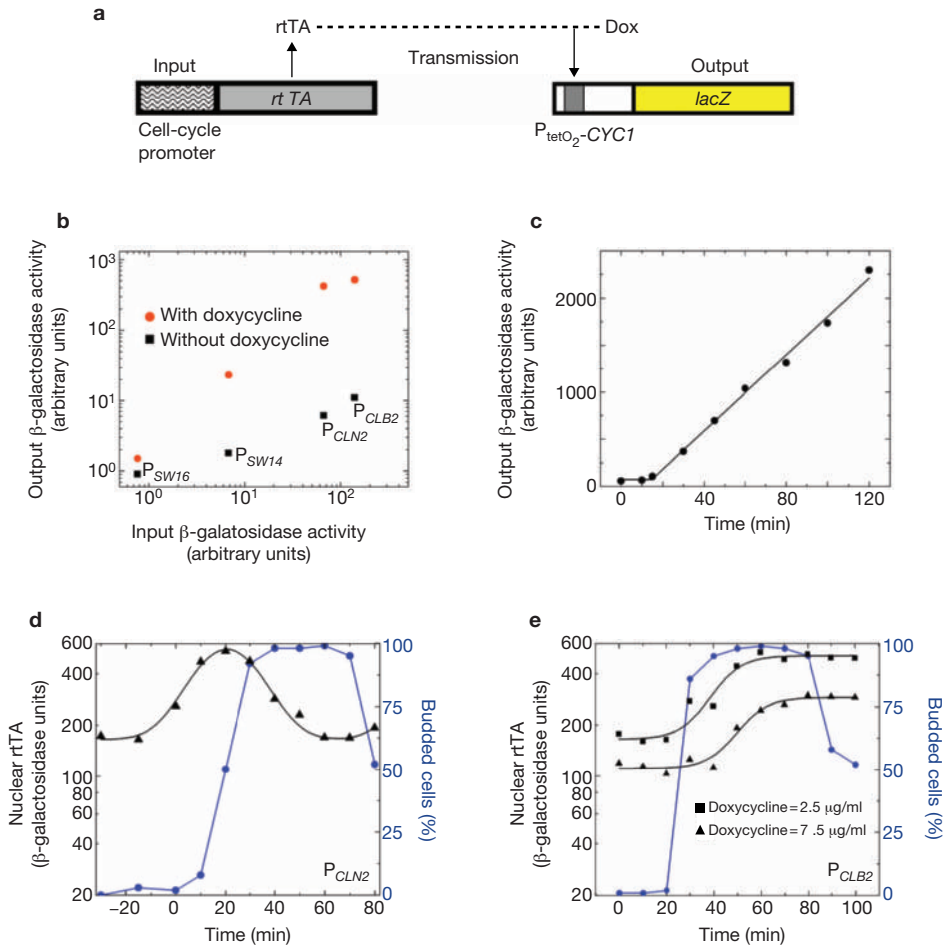

Figure 1 Constructs and properties of the transmission process. (**a**) The input and output genetic constructs were integrated at the *ade2* and *ura3* loci, respectively. (**b**) The β-galactosidase activities of input and output promoters. The input value corresponds to β-galactosidase activity when *lacZ* is expressed under the direct control of cell-cycle promoters (ABY0400–0403), whereas the output value corresponds to that when *lacZ* expression is under the control of rtTA (induced by 2.5 μg ml^{-1} doxycycline for 2 h) driven by the corresponding cell-cycle promoter (ABY0410–0413). Without doxycycline induction (black squares), the output β-galactosidase activity reflects background activation by rtTA at different expression levels, whereas in the presence of doxycycline, it increases by about two orders of magnitude (orange circles). (**c**) Induction kinetics of *lacZ* expression under the control of P_{CLB2}-rtTA after addition of 2.5 μg ml^{-1} doxycycline. (**d**, **e**) Output activities (black triangles, left ordinate) driven by *CLN2* and *CLB2* promoters (ABY0217, ABY0216) during cell-cycle progression. Time points indicate the moment of addition of doxycycline (2.5 μg ml^{-1}) when the budding index was determined (blue circles, right ordinate). Time points for 30, 15 min before and immediately after release from α-factor arrest are denoted as –30, –15 and 0 min.

After nuclear import of rtTA, it is ubiquitinylated by the nuclear ubiquitin ligase complex, SCF^{Met30}. The consequent degradation of the nuclear rtTA is likely to be a fast process because the VP16 activator domain confers a short half-life to transcriptional activators (~ 4 min for LexA-VP16) (ref. 14). The second component, nuclear rtTA, induces the transcription of the third component, the *lacZ* mRNA. Parameters that reduce the PTR and delay the phase of propagated waves describe processes that lower the activities of components in a cellular compartment, either by degradation, deactivation or depletion. Interestingly, accumulation processes (for example, increasing the rate of transcription) do not affect the phase and PTR of propagated waves. Nuclear import is unique in kinetic terms because it occurs as both a cytoplasmic depletion and nuclear accumulation process. Although increasing nuclear import rates have been found to shorten the period of biorhythmic oscillations[3], the analysis shows that increasing import rates are expected to augment the PTRs of oscillations (Fig. 2b) without lowering the overall intensity of waves, in contrast to rapid proteolysis, for example. Rapid degradation would not allow high PTR oscillations of low-copy mRNAs and proteins with low rates of synthesis. An initial PTR of 13.4 of a model input wave, which resembles the activity of the *CLN2* promoter, is reduced to 12.6 for nuclear rtTA when import is fast ($t_{1/2}$=1.4 min) and to 4.3 at a ten-fold slower import rate. The phase delay associated with the slower transport is three times longer compared with the faster one (Fig. 2 d, e). From the analysis above, it is expected that increasing the import rate of rtTA should counteract the reduction of the PTR of nuclear rtTA oscillations (Fig. 2e).

In the next step, rtTA was tagged with nuclear localization sequences (NLSs). The viral SV40NLS and the yeast CBP80NLS were selected. CBP80NLS binds stronger to the import receptor than SV40NLS, and it is possibly the highest affinity NLS in yeast[15]. The relative import rates of untagged and NLS-tagged rtTA–green fluorescent protein

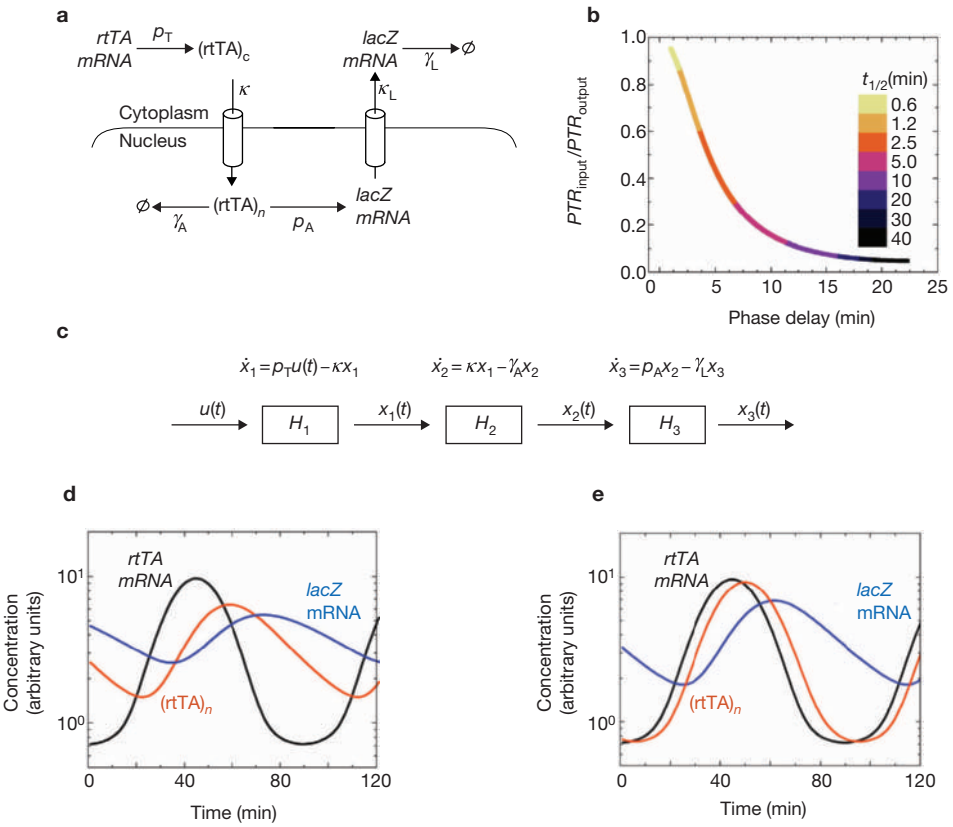

Figure 2 Mathematical analysis of propagation of transcriptional oscillations. (**a**) Elementary steps with rate constants participating in the transmission process depicted in Fig. 1a are discussed in Methods. (**b**) Reduction of PTR (defined as PTR_{input}/PTR_{output}) (see equation 2) and phase shift were calculated for a single-step process with a sinusoidal input wave (B_0=1.1, B_1=1). The half-time of the reduction process (γ) was varied between 0.6 and 50 min and represented by colour coding. (**c**) Block diagrams representing the wave transmission process. (**d**, **e**) Solutions of equation 1 for nuclear rtTA and *lacZ* mRNA with the following parameter values: B_0=0.36, B_1= –0.42, B_2 = 0.16 and B_3 = –0.028. T = 90 min, p_T = 0.3 min^{-1}, p_A = 0.05 min^{-1}. Half-times of slow and fast import are 13.8 min (**d**) and 1.4 min (**e**), whereas half-lives of nuclear rtTA and *lacZ* mRNA are 2.3 min and 17.3 min, respectively. The PTRs of the *lacZ* mRNA are 2 (**d**) and 3.4 (**e**).

(GFP) constructs were inferred from the ratio of nuclear to cytoplasmic fluorescence. Ratios of 1.8, 6.0 and 9.9 were found for untagged, SV40NLS- and CBP80NLS-tagged constructs, respectively (Fig. 3a), reflecting the high affinity of CBP80NLS for the import receptor.

Because GFP-fusion proteins often have longer half-lives, the fluorescence of rtTA–GFP fusions does not follow the high PTR oscillations of nuclear rtTA. Therefore, we used the transient *lacZ* induction scheme, to measure the PTR of nuclear rtTA. A computational simulation confirms that the transient induction technique is able to detect changes in the PTR of nuclear rtTA as its import rate increases (Supplementary Information, Fig. S1). This technique relies on the short half-life and appropriate induction period of rtTA, and is independent of the stability of *lacZ* mRNA. To measure the PTR of the third component of wave propagation, *lacZ* mRNA was quantified after its transcription was allowed to proceed continuously in the presence of doxycycline.

The PTR of waves reflecting nuclear rtTA-SV40NLS and CBP80NLS-rtTA increased by about a factor of 2 and 3.5, respectively, compared with the transmission using untagged rtTA (Fig. 3b–e). These results are consistent with the predictions of the previous analysis, showing that increasing rates of import counteract the reduction of PTR. The temporal evolution of the waves did not change considerably, although the waves generated by rtTA-SV40NLS and CBP80NLS-rtTA were narrower. The import of CBP80NLS-rtTA by a two-step mechanism might increase the delay of the response wave without compromising its PTR (see Methods).

To determine the PTR of the input wave, *rtTA* mRNA level was measured. Expression of *rtTA* mRNA under the control of *CLN2* promoter peaks before the onset of budding, with a PTR of approximately 11 (Fig. 4 a, b), in agreement with the expression pattern of *CLN2* mRNA[11]. Therefore, after a two-step transmission process, the PTR of nuclear CBP80NLS-rtTA oscillations is similar to that of the input oscillations, whereas the PTR of nuclear rtTA, without NLS tag, is a factor of four smaller than the PTR of the input.

Interestingly, the PTRs of the *lacZ* mRNA waves were reduced uniformly to values between 2 and 2.7 for all three rtTA constructs (Figs 4c–e and 5a). The simulations (Fig. 2d, e) show that when oscillations of nuclear rtTA propagate to the third component of the transmission process, *lacZ* mRNA, the relatively long half-life of mRNA (17 min) counteracts the effect of the higher rates of nuclear import. This explains why the contrast between the PTRs of the *lacZ* mRNA waves is smaller than that for the respective nuclear rtTA constructs.

A rapid increase of *CLN2* promoter activity occurs between 0 and 10 min after release from α-factor arrest, whereas the corresponding rapid increase in the transcription of *lacZ* occurred 20–25 min later. The phase of the output wave with the untagged rtTA transmission module is slightly delayed (~ 7 min) compared with the waves transmitted by NLS-tagged rtTAs (Fig. 4). Because the transmission of a

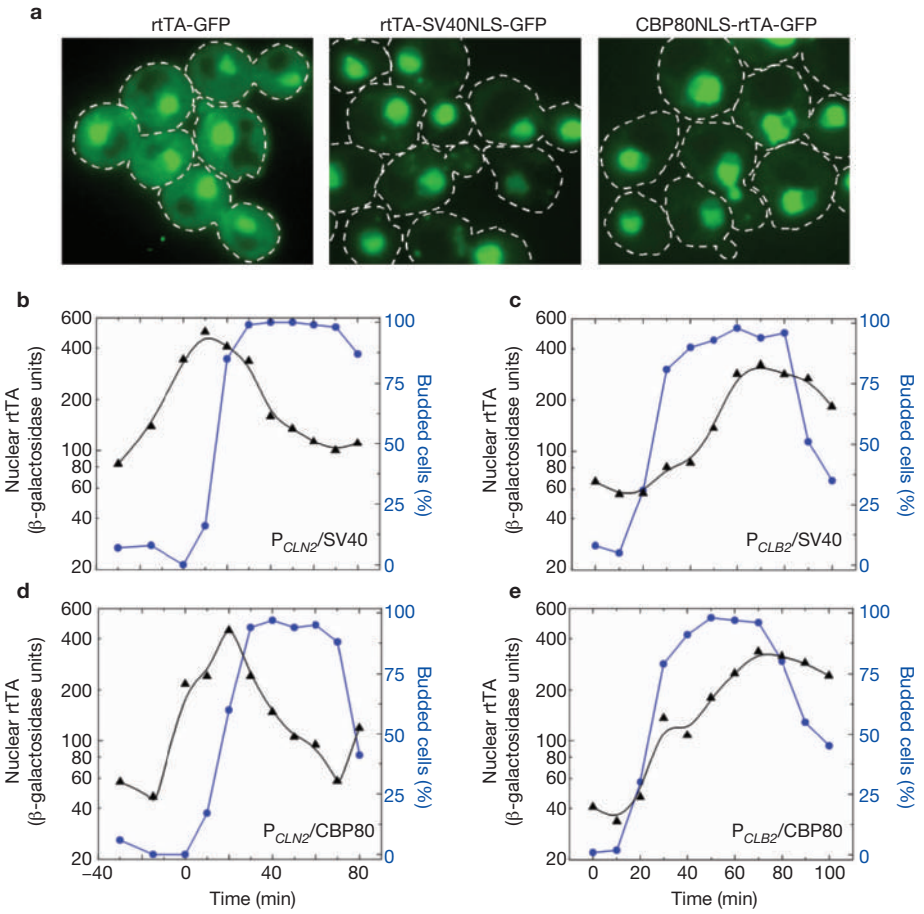

Figure 3 Import rates of rtTA constructs and their effect on the PTR of the transmitted waves. Lines are guides to the eye. (**a**) Localization of untagged and SV40NLS- and CBP80NLS-tagged rtTA-GFP fusion proteins expressed under the control of P_{CLB2} in strains ABY0435, ABY0437 and ABY0439. The respective means and standard deviations of their nucleocytoplasmic ratios are 1.8 ± 0.4, 6.0 ± 2.1 and 9.9 ± 2.2. Dashed lines indicate the cell perimeter as obtained by phase-contrast microscopy. (**b**, **c**) For the rtTA-SV40NLS transmission module with 2.5 μg ml^{-1} doxycycline induction, PTR_{CLN2} = 6.0±0.9 (ABY0221) and PTR_{CLB2} = 6.2±0.5 (ABY0224). For comparison, PTR_{CLN2} = 2.9±0.6 and PTR_{CLB2} = 3.0±0.3 for the untagged rtTA (Fig. 1). Mean values and standard deviations are calculated from three experiments. (**d**, **e**) For CBP80NLS-rtTA, PTR_{CLN2} = 11.4±2.5 (ABY0224) and PTR_{CLB2} = 10.8±2.0 (ABY0243). For induction, 25 μg ml^{-1} of doxycycline was used to match transcription activity of CBP80NLS-rtTA with that of rtTA and rtTA-SV40NLS (see Supplementary Information, Fig. S2). Blue circles refer to budding index and black triangles refer to nuclear rtTA level.

wave of transcriptional activity from one promoter to another lasts 20–25 min, the 90-min period of the yeast cell cycle can accommodate four such transmission processes. This observation is consistent with the finding that the sequential activation of cell-cycle transcriptional regulators is arranged in three to four major stages during the progression of the cell cycle[5].

Waves propagated in the synthetic gene circuit demonstrate the effect of different cellular processes and kinetic parameters relevant to the cell cycle. Varying nuclear transport rates lead to either strong nuclear localization (for example, Cln3) or a more homogeneous nuclear–cytoplasmic distribution (for example, Cln2) (ref. 16) of cell-cycle regulators (compare with Fig. 3a). Cell-cycle regulators are often degraded by the nuclear ubiquitin-ligase pathways. Most mRNAs, including cell-cycle regulator mRNAs, have half-lives close to the average mRNA half-life (17–23 min) (ref. 17), comparable to that of *lacZ* mRNA (17 min; Fig. 4, and see Supplementary Information). Therefore, analysis of how different cellular processes affect wave propagation in the gene circuit allows their kinetic classification with respect to wave propagation in the yeast cell-cycle network. Waves can be propagated with high fidelity during fast nuclear translocation and proteolysis steps (Fig. 5a). Surprisingly, a substantial (five- to sixfold) reduction of PTR occurs at the final step of a one-stage transcriptional activation process (Fig. 5a), within one-quarter of the cell-cycle period. This reduction occurs because of the characteristic turnover rate of yeast mRNAs. Nuclear transport has a very broad regulatory range and controls the phase and PTR of waves without change in their mean intensity. These specific properties enable nuclear transport to set time delays and to propagate cell-cycle waves with higher fidelity. A one-step process that transmits waves with high PTRs generates a short phase delay (Fig. 2b), which might be insufficient to separate cell-cycle stages. Intriguingly, a transmission module with multiple fast steps (involving, for example, nuclear transport) generates output waves with a small reduction in PTR and a long delay, comparable to the duration of one cell-cycle stage (Fig. 5b). In contrast, a module with fewer and slower steps (involving, for example, transcription) results in significantly lower PTRs for the same delay (Fig. 5b). This possibly explains why progression through even a single stage of the cell cycle is mediated by a sequence of multiple, fast cellular processes that preserve the intensity of waves. An example of

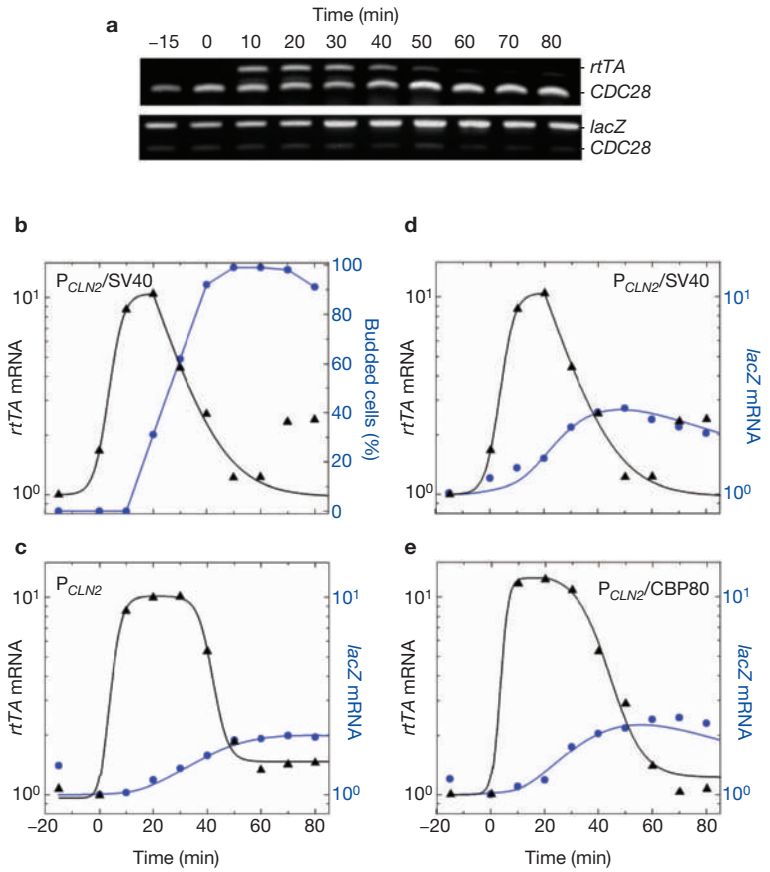

Figure 4 Transcript levels of untagged and NLS-tagged P_{CLN2}-*rtTA*, and $P_{TETO2CYC1}$-*lacZ* genes. Thirty minutes after addition of α-factor, doxycycline was added to the culture medium and was present throughout the arrest and also after release. (**a**) cDNA amplified from *CBP80NLS-rtTA* and *lacZ* mRNAs along with *CDC28* mRNA for normalization. (**b**) P_{CLN2}-*rtTA-SV40NLS* expression (black triangles) precedes the onset of budding (blue circles). (**c**) *rtTA* (**d**) *SV40NLS-rtTA* (**e**) *CBP80NLS-rtTA* mRNAs (black triangles) and the corresponding *lacZ* mRNA. All values were normalized to the mRNA level at –15 min. *lacZ* mRNA levels were fitted by the output of the three-step transmission module (see Methods) by using *rtTA* mRNA levels as input. Values for fitted parameters are $\gamma_A = 0.3$ min^{-1}, $\gamma = 0.04$ min^{-1} (half-life = 17 min). Relative values are given for κ, because in the range of fast import rates, the import rates can be varied considerably, with small changes in the phase shift (less than 4 min). The fitted values for κ indicate that the import rate of the NLS-tagged rtTA is at least four times higher than that of the untagged rtTA. The PTRs for *rtTA*, *rtTA-SV40NLS* and *CBP80NLS-rtTA* mRNAs are 10.1, 10.4 and 11.7, and for the corresponding *lacZ* mRNAs 2, 2.7 and 2.5, respectively.

this principle is the mitotic exit, where oscillatory signals propagate through a sequence of multiple nuclear translocation events[4] (see Supplementary Information).

The cell-cycle oscillator can be considered as a network of interconnected wave propagation modules. Therefore, classification of cellular processes in terms of phase and amplitude control (Fig. 5) will help the identification of appropriate strategies for amplification of oscillations and setting time delays in different circuits of the cell-cycle oscillator[18–20].

High- and low-fidelity wave propagation modules (Fig. 5b, blue and red lines, respectively) are expected to be embedded in different regulatory network motifs of the cell cycle. For example, in addition to nuclear translocation cascades of the mitotic exit network, kinase cascades are likely to propagate waves with long delay and high fidelity (Fig. 5b). Such a mechanism might underlie the delayed activation of the anaphase-promoting complex (APC) by Clb2 in the cell-cycle core oscillator. Conversely, linear transcriptional networks display low-fidelity propagation of cell-cycle waves (Fig. 5a). Therefore, it is crucial that even a one-stage transcriptional activation process is coupled to mechanisms that amplify or sharpen transitions in oscillations, such as ultra-sensitive switches, appropriate combination of feedback loops, and regulation by the core oscillator, such as periodic proteolysis[21–24]. For example, positive feedback loops in *CLB2* expression and periodic Clb2 degradation[25] are likely mechanisms underlying the substantial amplification of the PTR of *CLB2* transcriptional oscillations (see Supplementary Information). Additionally, *CLB2* mRNA has been shown to be degraded periodically[26], which might further increase the PTR of mRNA oscillations. The synergy of these mechanisms might explain why the PTR of the output transcriptional oscillation (14 for *CLB2* mRNA) can be higher than that of the regulating transcriptional factors (2 for *NDD1* mRNA) (ref. 11). The ultrasensitive switch, by which Sic1 is degraded after its multi-site phosphorylation by Cln2-Cdc28, provides another mechanism that can amplify oscillations[24]. Reconstruction of various steps of wave propagation will be essential to isolate the contribution of various mechanisms to robust cell cycle and biorhythmic oscillations. □

METHODS

Mathematical analysis. Our model focuses on a linear sequence of elementary processes by which a eukaryotic transcriptional activator transmits oscillatory

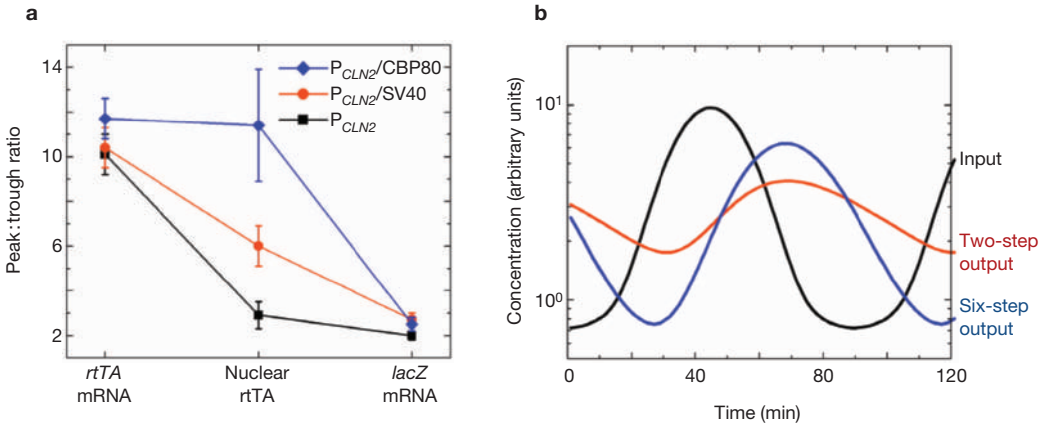

Figure 5 Attenuation of oscillations during the transmission process. (**a**) PTRs are shown for *rtTA* mRNA, nuclear rtTA and *lacZ* mRNA waves, which correspond to the input, the second and third component of the transmission process. Data are obtained from Figs 1, 3 and 4. (**b**) The input wave corresponds to *rtTA* mRNA waves in Fig. 2d, e. For the two-step process, the half-time of the reduction process is 13.9 min and for the six-step process 2.9 min, which is in the range relevant to nuclear transport (0.1–15 min) (refs 27–29). Within each of a two- or six-step transmission process, rate constants for accumulation are equal to those of reduction processes as in nuclear transport (see Methods) or in other processes (for example, kinase–phosphatase cascades) that preserve the mean during wave propagation. In both transmission processes the delay between the input and output wave is 24 min, which roughly corresponds to one cell-cycle stage. The PTR of the input (13.4) is reduced to 2.3 and 8.4 for the two- and six-step processes, respectively.

activity from an input promoter to an output promoter (Fig. 2a). The three main components in this sequence are modelled by first-order reactions, with rate constants given in parentheses.

(1) Cytoplasmic rtTA, x_1, results from translation of *rtTA* mRNA (p_T) and NLS-tagged rtTA is imported into the nucleus at constant rate by Kap95/Kap60 (refs 30 and 31) (κ).

(2) During nuclear import of protein cargoes, the cargo binds to the receptor and diffuses through the nuclear pore complex (NPC). The rate-limiting process is likely to be rate of association of the cargoes with receptors[30]. In comparison, the diffusion of receptor–cargo complexes is fast[28]. Therefore, the rate of transport is proportional to the receptor cargo association rate[27]. The ubiquitinylated nuclear rtTA, x_2, activates transcription and is subsequently degraded (γ_A) (ref. 14).

(3) rtTA activates the transcription (p_A) of *lacZ* mRNA, x_3. Nuclear export of mRNA (κ_L) is likely to be fast[32], therefore it is not included in this model explicitly. Nuclear and cytoplasmic degradation of *lacZ* mRNA is described by the lumped parameter γ_L.

The three steps are represented by a chain of block diagrams with the corresponding linear differential equations above (Fig. 2c). The input $u(t)$ is a periodic function reflecting the *rtTA* mRNA concentration. The Laplace transform (the kernel wherein is e^{-st}) of the output x_3 can be written as:

$$X_3(s) = PH_1(s)H_2(s)H_3(s)U(s)$$

$$H_1(s) = \frac{1}{\kappa+s} \qquad H_2(s) = \frac{1}{\gamma_A+s} \qquad H_3(s) = \frac{1}{\gamma_L+s}$$

The input $u(t)$ is represented by a Fourier cosine series consisting of the terms $B_m\cos(m\omega t)$, $m = 0,1,2,\ldots,\infty$. $\omega = 2\pi/T$, where T is the cell doubling time. $U(s)$ is the Laplace transform of $u(t)$. The transfer functions $H(s)$ determine to what extent the degradation and transport terms shift the phase, by $\arg(H(im\omega))$, and scale the amplitude, by $|H(im\omega)|$, of the propagating wave at each step of the transmission. The accumulation terms p_T, κ, p_A scale the output linearly: $P = p_T\kappa p_A$. In this case, the long-term solution for the three-step process is given by inverting the Laplace transforms.

$$x_3(t) = \sum_{m=0}^{\infty} B_m P \prod_{z=1}^{3} |H_z(im\omega)| \times \cos\left\{m\omega t + \sum_{z=1}^{3} \arg(H_z(im\omega))\right\} \qquad (1)$$

For a sinusoidal input wave with amplitude B_1 and background B_0, the phase of the output after the first step is delayed by $\varphi = \arctan(\omega/\kappa)$ and its PTR is reduced owing to the factor $|H_1(i\omega)|/|H_1(0)| = \kappa/(\kappa^2+\omega^2)^{1/2} \leq 1$:

$$PTR = \left(B_0 + B_1 \frac{\kappa}{\sqrt{\omega^2+\kappa^2}}\right) / \left(B_0 - B_1 \frac{\kappa}{\sqrt{\omega^2+\kappa^2}}\right) \qquad (2)$$

From the above equations the following conclusions can be drawn.

(1) Both the phase shift and PTR of the output are determined by the period of oscillations and the reduction terms (κ, γ_A, γ_L). The accumulation terms scale the output only linearly. The amplitudes of waves are multiplied by the absolute value of the transfer function at each step. κ is not a factor of B_0 in x_2; therefore varying the import rate preserves the mean value of nuclear rtTA concentration.

(2) The delay between the input and output wave (phase-shift) is increased by each step in an additive way.

(3) When, in addition to association, the dissociation rate of receptor–cargo complexes is rate limiting[30], nuclear import can be described by two linear equations for association and dissociation of receptor–cargo complexes, because their motion within the NPC is random[27]. The relatively slow dissociation of CBP80NLS from the import receptor[15] might result in a two-step import. The PTR of the response wave is higher with import involving two fast steps than with import involving one slower step, although the associated phase-shifts may be equal (Fig. 5b, see also Supplementary Information).

Construction of plasmids and strains. *Sal*I-promoter-*Bam*HI, *Bam*HI-rtTA-*Bsr*GI, *Bam*HI-lacZ-*Xba*I fragments were cloned into pRS306 or pRS402 backbones upstream of a *CYC1* transcriptional terminator. The P_{SWI6}, P_{SWI4}, P_{CLN2} and P_{CLB2} promoter sequences correspond to 600, 1360, 1114 and 1995 base pair regions upstream of the start codon of the respective genes. $P_{TETO2\text{-}CYC1}$ corresponds to tetreg promoter[13]. CBP80NLS corresponds to the N-terminal 33 amino acids of CBP80 and was inserted in the *Bam*HI site. For construction of rtTA-SV40NLS the C-terminal glycine of rtTA was fused to the AGAPP-KKKRKVAGI amino-acid sequence. For rtTA GFP fusions, the *Eco*NI-*Sph*I fragment of TetR-GFP-VP16 fusion proteins[13] was transferred into the untagged and NLS-tagged rtTA constructs under the control of P_{CLB2}.

All strains were derivatives of W303. Strains ABY0400-0403 contain P_{SWI6}-*lacZ*, P_{SWI4}-*lacZ*, P_{CLN2}-*lacZ*, P_{CLB2}-*lacZ* constructs inserted at the *ade2* locus in a MATa/(*ura3/ura3*::*URA3* background, respectively. The ABY0410–0413

strains contain insertions of the P_{SWI6}-*rtTA*, P_{SWI4}-*rtTA*, P_{CLN2}-*rtTA*, P_{CLB2}-*rtTA* constructs at *ade2* locus in a MATa/α *ura3/ura3*::*URA3*-$P_{TETO2\text{-}CYC1}$-*lacZ* background, respectively. Multiple integration of pRS306-$P_{TETO2\text{-}CYC1}$-*lacZ* (between 5 and 10 copies, determined as in ref. 13) in a MATa background resulted in ABY0062. Insertion of P_{CLB2}-*rtTA-SV40NLS*, P_{CLB2}-*rtTA*, P_{CLN2}-*rtTA*, P_{CLN2}-*rtTA-SV40NLS*, P_{CLN2}-*CBP80NLS-rtTA* and P_{CLB2}-*CBP80NLS-rtTA* constructs at the *ade2* locus of ABY0062 resulted in ABY0214, ABY0216, ABY0217, ABY0221, ABY0224 and ABY0243 strains, respectively.

Growth conditions and α-factor synchronization. Yeast cells were grown in YeP-D (2% glucose) medium at 30 °C. Exponentially growing cells were diluted to optical density at 600 nm (OD_{600}) of 0.2 and cells were arrested in G1 with 5 μg ml^{-1} α-factor. Cells were released by washing out α-factor. When the percentage of budded cells was higher than 80%, α-factor was re-added to temporarily halted cell-cycle progression at G1, circumventing the effect of differential duration of G1 phase in mother and daughter cells on *lacZ* expression. Samples were taken at the time of doxycycline addition to determine the budding index (number of budded cells among a total of a 100 cells) by using light microscopy, whereas samples for measurement of β-galactosidase activity were taken 30 min after doxycycline induction.

Reverse transcription–polymerase chain reaction. Total RNA was isolated by RiboPure Yeast Kit (Ambion). Concentrations were adjusted to 200 ng μl^{-1}, and 200 ng of total RNA was used in 40 μl reaction with Stratascript RT and TaqPlus Precision (Stratagene). Twenty to 21 and 26 to 27 polymerase chain reaction cycles were performed for the detection of *lacZ* and *rtTA* mRNAs, respectively. *CDC28* mRNA was used to normalize the values of *rtTA* and *lacZ* mRNAs. cDNA was quantified after ethidium bromide staining, UV irradiation and image acquisition by charge-coupled device camera.

Note: Supplementary Information is available on the Nature Cell Biology website.

ACKNOWLEDGEMENTS

We are indebted to A. Amon at the Center for Cancer Research, Massachusetts Institute of Technology, for discussions throughout the progress of this work and for her support to M.G.B. We thank H. Blitzblau, I. W. Mattaj and A. Varshavsky for discussions, and W. Hillen for the rtTA(S2) construct. A.B. is a Long Term Fellow of the Human Frontiers Science Program. This work was supported by a grant from the National Institutes of Health (grant GM068957).

COMPETING FINANCIAL INTERESTS

The authors declare that they have no competing financial interests.

Received 1 March 2004; accepted 25 March 2004
Published online at http://www.nature.com/naturecellbiology

1. Georgi, A. B., Stukenberg, P. T. & Kirschner, M. W. Timing of events in mitosis. *Curr. Biol.* **12,** 105–114 (2002).
2. Moll, T., Tebb, G., Surana, U., Robitsch, H. & Nasmyth, K. The role of phosphorylation and the CDC28 protein kinase in cell cycle-regulated nuclear import of the *S. cerevisiae* transcription factor SWI5. *Cell* **66,** 743–758 (1991).
3. Martinek, S., Inonog, S., Manoukian, A. S. & Young, M. W. A role for the segment polarity gene shaggy/GSK-3 in the *Drosophila* circadian clock. *Cell* **105,** 769–779 (2001).
4. Stegmeier, F., Visintin, R. & Amon, A. Separase, polo kinase, the kinetochore protein Slk19, and Spo12 function in a network that controls Cdc14 localization during early anaphase. *Cell* **108,** 207–220 (2002).
5. Simon, I. *et al.* Serial regulation of transcriptional regulators in the yeast cell cycle. *Cell* **106,** 697–708 (2001).
6. Breeden, L. L. Cyclin transcription: timing is everything. *Curr. Biol.* **10**, R586–R588 (2000).
7. Tanaka, S. & Diffley, J. F. Deregulated G1-cyclin expression induces genomic instability by preventing efficient pre-RC formation. *Genes Dev.* **16,** 2639–2649 (2002).
8. MacKay, V. L., Mai, B., Waters, L. & Breeden, L. L. Early cell cycle box-mediated transcription of CLN3 and SWI4 contributes to the proper timing of the G(1)-to-S transition in budding yeast. *Mol. Cell. Biol.* **21,** 4140–4148 (2001).
9. Strohmaier, H. *et al.* Human F-box protein hCdc4 targets cyclin E for proteolysis and is mutated in a breast cancer cell line. *Nature* **413,** 316–322 (2001).
10. Urlinger, S. *et al.* Exploring the sequence space for tetracycline-dependent transcriptional activators: novel mutations yield expanded range and sensitivity. *Proc. Natl Acad. Sci. USA* **97,** 7963–7968 (2000).
11. Spellman, P. T. *et al.* Comprehensive identification of cell cycle-regulated genes of the yeast Saccharomyces cerevisiae by microarray hybridization. *Mol. Biol. Cell* **9,** 3273–3297 (1998).
12. Bachmair, A. & Varshavsky, A. The degradation signal in a short-lived protein. *Cell* **56,** 1019–1032 (1989).
13. Becskei, A., Seraphin, B. & Serrano, L. Positive feedback in eukaryotic gene networks: cell differentiation by graded to binary response conversion. *EMBO J.* **20,** 2528–2535 (2001).
14. Salghetti, S. E., Caudy, A. A., Chenoweth, J. G. & Tansey, W. P. Regulation of transcriptional activation domain function by ubiquitin. *Science* **293,** 1651–1653 (2001).
15. Gorlich, D. *et al.* Importin provides a link between nuclear protein import and U snRNA export. *Cell* **87,** 21–32 (1996).
16. Edgington, N. P. & Futcher, B. Relationship between the function and the location of G1 cyclins in *S. cerevisiae*. *J. Cell Sci.* **114,** 4599–4611 (2001).
17. Wang, Y. *et al.* Precision and functional specificity in mRNA decay. *Proc. Natl Acad. Sci. USA* **99,** 5860–5865 (2002).
18. Thornton, B. R. & Toczyski, D. P. Securin and B-cyclin/CDK are the only essential targets of the APC. *Nature Cell Biol.* **5,** 1090–1094 (2003).
19. Sveiczer, A., Csikasz-Nagy, A., Gyorffy, B., Tyson, J. J. & Novak, B. Modeling the fission yeast cell cycle: quantized cycle times in wee1–cdc25Delta mutant cells. *Proc. Natl Acad. Sci. USA* **97,** 7865–7870 (2000).
20. Cross, F. R. Two redundant oscillatory mechanisms in the yeast cell cycle. *Dev. Cell* **4,** 741–752 (2003).
21. Breeden, L. L. Periodic transcription: a cycle within a cycle. *Curr. Biol.* **13,** R31–R38 (2003).
22. Hasty, J., Dolnik, M., Rottschafer, V. & Collins, J. J. Synthetic gene network for entraining and amplifying cellular oscillations. *Phys. Rev. Lett.* **88,** 148101 (2002).
23. Pomerening, J. R., Sontag, E. D. & Ferrell, J. E. Jr Building a cell cycle oscillator: hysteresis and bistability in the activation of Cdc2. *Nature Cell Biol.* **5,** 346–351 (2003).
24. Nash, P. *et al.* Multisite phosphorylation of a CDK inhibitor sets a threshold for the onset of DNA replication. *Nature* **414,** 514–521 (2001).
25. Amon, A., Tyers, M., Futcher, B. & Nasmyth, K. Mechanisms that help the yeast cell cycle clock tick: G2 cyclins transcriptionally activate G2 cyclins and repress G1 cyclins. *Cell* **74,** 993–1007 (1993).
26. Gill, T., Cai, T., Aulds, J., Wierzbicki, S. & Schmitt, M. E. RNase MRP cleaves the CLB2 mRNA to promote cell cycle progression: novel method of mRNA degradation. *Mol. Cell Biol.* **24,** 945–953 (2004).
27. Becskei, A. & Mattaj, I. W. The strategy for coupling the RanGTP gradient to nuclear protein export. *Proc. Natl Acad. Sci. USA* **100,** 1717–1722 (2003).
28. Ribbeck, K. & Gorlich, D. Kinetic analysis of translocation through nuclear pore complexes. *EMBO J.* **20,** 1320–1330 (2001).
29. Shulga, N. *et al.* In vivo nuclear transport kinetics in *Saccharomyces cerevisiae*: a role for heat shock protein 70 during targeting and translocation. *J. Cell Biol.* **135,** 329–339 (1996).
30. Gilchrist, D., Mykytka, B. & Rexach, M. Accelerating the rate of disassembly of karyopherin.cargo complexes. *J. Biol. Chem.* **277,** 18161–18172 (2002).
31. Makhnevych, T., Lusk, C. P., Anderson, A. M., Aitchison, J. D. & Wozniak, R. W. Cell cycle regulated transport controlled by alterations in the nuclear pore complex. *Cell* **115,** 813–823 (2003).
32. Audibert, A., Weil, D. & Dautry, F. In vivo kinetics of mRNA splicing and transport in mammalian cells. *Mol. Cell Biol.* **22,** 6706–6718 (2002).

SUPPLEMENTARY INFORMATION
Amplitude control of cell cycle waves by nuclear import

SUPPLEMENTARY DISCUSSION

Comparison of kinetic parameters of synthetic transmission circuit and cell cycle network

Nuclear transport

Transcription factors perform their role after being imported into the nucleus at a rate determined by their NLSs, their diffusion coefficient and the modifications of the NPC[1]. Import of Swi5 is regulated by phosphorylation which contributes to dynamical response by Swi5[2]. The proper functioning of Swi6 requires both import and export activities, which confers a continuous shuttling to Swi6[3]. Cyclins also display varying ratios of nuclear-cytoplasmic distribution. Cln3 is primarily localized to the nucleus via a bipartite NLS while Cln2 localizes both to the cytoplasm and nucleus[4,5]. Clb2 is primarily nuclear, its import is mediated by a bipartite NLS. Mutation of a nuclear export like sequence (NES) in *CLB2* enhances its nuclear localization.

rtTA alone has weak import activity (Fig 3a), possibly due to a weak NLS-like sequence in TetR-VP16. The bacterial transcription factor LexA contains an NLS-like sequence[6]. It is likely that NLS like sequences in prokaryotes have no role in the natural context of the protein. CBP80NLS is possibly the strongest NLS in yeast[7]. Therefore, the import rate of different rtTA constructs ranges from slow to very fast.

Proteolysis

The G1 cyclins (Cln1, Cln2 and Cln3) are degraded by the SCF^{Grr1} pathway. The reported half-lives for G1 cyclins is between 3 and 10 min[8-10]. In comparison LexA-VP16 is degraded by SCF^{Met30} with a half-life of 4 min[11]. GFP constructs tagged with degradation signals often have longer half-lives (see e.g. ref [12] and references therein) in comparison to other proteins. This might account for the observation that rtTA-GFP fusion proteins do not follow the high PTR oscillations of nuclear rtTA.

Half-life of mRNAs

Half-life of mRNAs[13] of various cell cycle regulators are given in the table below. Cell cycle transcription regulators are typed boldface. These values are close to the average yeast mRNA half-life (17-23 min). The half-life for *lacZ* mRNA obtained from the least squares data analysis in Fig. 4 is 17 min. The same half-life was used in the equation for *lacZ* mRNA in Fig. 2 c,d. Histone mRNAs have short-half lives (~ 7 min)[14] and their stability displays periodicity. These factors may account for the high PTR of the histone transcript oscillations[15].

Phase and PTR of waves generated by CBP80NLS-rtTA.

The phase of *lacZ* mRNA waves elicited by rtTA tagged with SV40NLS or CBP80NLS is advanced in comparison to waves elicited by the untagged rtTA construct (Fig. 4c-e). The phase delay of the *lacZ* mRNA wave elicited by CBP80NLS-rtTA is longer than the delay predicted from the experimentally observed high PTR of nuclear CBP80NLS-rtTA (Fig. 3d-e) using Eq. 1. This can be explained by the two-step model of nuclear transport. The dissociation of CBP80NLS from the import receptor is slower than that of SV40NLS[16]. For rtTA and rtTA-SV40NLS only the association is likely to be the rate-limiting step, while for CBP80NLS-rtTA both association and dissociation of receptor cargo-complexes might be rate limiting. The rates of the two processes are still expected to be considerably higher than, for example, the average of mRNA half-life. The import of CBP80NLS-rtTA involving two fast processes is expected to generate a response wave with a higher PTR than an import involving one slower process (i.e. the slower association of SV40NLS). However, the associated phase-delays are similar for both transmission processes (Fig 5b).

Amplitude control of *CLB2* mRNA expression.

Expression of *CLB2* mRNA is regulated by transcriptional factors Ndd1 and Fkh2. *NDD1*and *FKH2* have weak oscillatory expression patterns, while Clb2 enhances its own expression since Clb2-Cdk1 phosphorylates and activates Ndd1[17,18]. Other mechanism might contribute to the expression of *CLB2*[18], as well. The three main components in the autoactivation loop are modeled based on the following processes, with rate constants given in parentheses:

(1) Expression of *CLB2* mRNA, x_1, is regulated by the basal periodic activity of Ndd1 and Fkh2, $f_{input}(t)p_{bas}$. The activity of Ndd1 increases linearly by phosphorylation by Clb2. Phosphorylated Ndd1 is assumed to bind cooperatively to the *CLB2* promoter, with a Hill coefficient *n,* effective binding constant *K* and maximum activation level *a*. The *CLB2* mRNA is degraded (γ) with a half-life of 13 min.

(2) Translation of mRNA (*p*) in the cytoplasm results in Clb2, x_2, which is imported into the nucleus (κ).

(3) The nuclear Clb2, x_3, phosphorylates Ndd1 and gets degraded by the periodic activity of the nuclear ubiquitin ligase complex, APC, $f_{APC}(t)$, with peak activity in anaphase and G1.

These reactions are reflected in the following model:

$$\dot{x}_1 = f_{input}(t)\left(p_{bas} + a\frac{x_3^n}{K + x_3^n} \right) - \gamma x_1$$

$$\dot{x}_2 = p x_1 - \kappa x_2$$

$$\dot{x}_3 = \kappa x_2 - f_{APC}(t) x_3$$

SUPPLEMENTARY REFERENCES:

1. Makhnevych, T., Lusk, C. P., Anderson, A. M., Aitchison, J. D. & Wozniak, R. W. Cell cycle regulated transport controlled by alterations in the nuclear pore complex. *Cell* **115**, 813-23 (2003).
2. Moll, T., Tebb, G., Surana, U., Robitsch, H. & Nasmyth, K. The role of phosphorylation and the CDC28 protein kinase in cell cycle-regulated nuclear import of the S. cerevisiae transcription factor SWI5. *Cell* **66**, 743-58 (1991).
3. Queralt, E. & Igual, J. C. Cell cycle activation of the Swi6p transcription factor is linked to nucleocytoplasmic shuttling. *Mol Cell Biol* **23**, 3126-40 (2003).
4. Edgington, N. P. & Futcher, B. Relationship between the function and the location of G1 cyclins in S. cerevisiae. *J Cell Sci* **114**, 4599-611 (2001).
5. Miller, M. E. & Cross, F. R. Mechanisms controlling subcellular localization of the G(1) cyclins Cln2p and Cln3p in budding yeast. *Mol Cell Biol* **21**, 6292-311 (2001).
6. Rhee, Y., Gurel, F., Gafni, Y., Dingwall, C. & Citovsky, V. A genetic system for detection of protein nuclear import and export. *Nat Biotechnol* **18**, 433-7 (2000).
7. Gilchrist, D., Mykytka, B. & Rexach, M. Accelerating the rate of disassembly of karyopherin.cargo complexes. *J Biol Chem* **277**, 18161-72 (2002).
8. Tyers, M., Tokiwa, G., Nash, R. & Futcher, B. The Cln3-Cdc28 kinase complex of S. cerevisiae is regulated by proteolysis and phosphorylation. *Embo J* **11**, 1773-84 (1992).
9. Salama, S. R., Hendricks, K. B. & Thorner, J. G1 cyclin degradation: the PEST motif of yeast Cln2 is necessary, but not sufficient, for rapid protein turnover. *Mol Cell Biol* **14**, 7953-66 (1994).
10. Barral, Y., Jentsch, S. & Mann, C. G1 cyclin turnover and nutrient uptake are controlled by a common pathway in yeast. *Genes Dev* **9**, 399-409 (1995).
11. Salghetti, S. E., Caudy, A. A., Chenoweth, J. G. & Tansey, W. P. Regulation of transcriptional activation domain function by ubiquitin. *Science* **293**, 1651-3 (2001).
12. Elowitz, M. B. & Leibler, S. A synthetic oscillatory network of transcriptional regulators. *Nature* **403**, 335-8 (2000).
13. Holstege, F. C. et al. Dissecting the regulatory circuitry of a eukaryotic genome. *Cell* **95**, 717-28 (1998).
14. Wang, Y. et al. Precision and functional specificity in mRNA decay. *Proc Natl Acad Sci U S A* **99**, 5860-5 (2002).
15. Spellman, P. T. et al. Comprehensive identification of cell cycle-regulated genes of the yeast Saccharomyces cerevisiae by microarray hybridization. *Mol Biol Cell* **9**, 3273-97 (1998).
16. Gorlich, D. et al. Importin provides a link between nuclear protein import and U snRNA export. *Cell* **87**, 21-32 (1996).
17. Amon, A., Tyers, M., Futcher, B. & Nasmyth, K. Mechanisms that help the yeast cell cycle clock tick: G2 cyclins transcriptionally activate G2 cyclins and repress G1 cyclins. *Cell* **74**, 993-1007 (1993).

18. Reynolds, D. et al. Recruitment of Thr 319-phosphorylated Ndd1p to the FHA domain of Fkh2p requires Clb kinase activity: a mechanism for CLB cluster gene activation. *Genes Dev* **17**, 1789-802 (2003).

Table S1. mRNA half-lifes

mRNA	half life (min)
Cdc6	20
Clb2	13
Cln2	10
Fkh1	12
Fkh2	13
lacZ	17
Mbp1	24
Sic1	17
Swi4	13
Swi5	17
Swi6	21

Table S2. Yeast plasmids

Name	Description
PABB01	pRS306 $P_{TETO2CYC1}$-*lacZ*
PABB02	pRS402 P_{SWI6}-*lacZ*
pABB03	pRS402 P_{SWI4}-*lacZ*
pABB04	pRS402 P_{CLN2}-*lacZ*
pABB05	pRS402 P_{CLB2}-*lacZ*
pABT01	pRS402 P_{SWI6}-*rtTA(S2)*
pABT02	pRS402 P_{SWI4}-*rtTA(S2)*
pABT03	pRS402 P_{CLN2}-*rtTA(S2)*
pABT04	pRS402 P_{CLB2}-*rtTA(S2)*
pABT05	pRS402 P_{CLN2}-*rtTA(S2)-SV40NLS*
pABT06	pRS402 P_{CLB2}-*rtTA(S2)-SV40NLS*
pABT07	pRS402 P_{CLN2}-*CBP80NLS-rtTA(S2)*
pABT08	pRS402 P_{CLB2}-*CBP80NLS-rtTA(S2)*
pABTG1	pRS402 P_{CLB2}-*rtT-GFP-A*
pABTG2	pRS402 P_{CLB2}-*rtT-GFP-A-SV40NLS*
pABTG3	pRS402 P_{CLB2}-*CBP80NLS-rtT-GFP-A*

Table S3. Yeast strains

Name	Genotype
ABY0014	MAT**a** *ura3::URA3*-$P_{TETO2\text{-}CYC1}$-*lacZ*
ABY0400	MAT**a**/α *ade2 / ade2::ADE2-*P_{SWI6}*-lacZ* *ura3 / ura3::URA3*
ABY0401	MAT**a**/α *ade2 / ade2*::ADE2-P_{SWI4}-*lacZ* *ura3 / ura3::URA3*
ABY0402	MAT**a**/α *ade2 / ade2*::ADE2-P_{CLN2}-*lacZ* *ura3 / ura3::URA3*
ABY0403	MAT**a**/α *ade2 / ade2*::ADE2-P_{CLB2}-*lacZ* *ura3 / ura3::URA3*
ABY0410	MAT**a**/α *ade2 / ade2*::ADE2-P_{SWI6}-*rtTA(S2) ura3 / ura3::URA3*-$P_{TETO2\text{-}CYC1}$-*lacZ*
ABY0411	MAT**a**/α *ade2 / ade2*::ADE2-P_{SWI4}-*rtTA(S2) ura3 / ura3::URA3*-$P_{TETO2\text{-}CYC1}$-*lacZ*
ABY0412	MAT**a**/α *ade2 / ade2*::ADE2-P_{CLN2}-*rtTA(S2) ura3 / ura3::URA3*-$P_{TETO2\text{-}CYC1}$-*lacZ*
ABY0413	MAT**a**/α *ade2 / ade2*::ADE2-P_{CLB2}-*rtTA(S2)ura3 / ura3::URA3*-$P_{TETO2\text{-}CYC1}$-*lacZ*
ABY0214	MAT**a** *ade2::ADE2*-P_{CLB2}-*rtTA(S2)-SV40NLS ura3::URA3*-$P_{TETO2\text{-}CYC1}$-*lacZ*
ABY0216	MAT**a** *ade2::ADE2*-P_{CLB2}-*rtTA(S2) ura3::URA3*-$P_{TETO2\text{-}CYC1}$-*lacZ*
ABY0217	MAT**a** *ade2::ADE2*-P_{CLN2}-*rtTA(S2) ura3::URA3*-$P_{TETO2\text{-}CYC1}$-*lacZ*
ABY0221	MAT**a** *ade2::ADE2*-P_{CLN2}-*rtTA(S2)-SV40NLS ura3::URA3*-$P_{TETO2\text{-}CYC1}$-*lacZ*
ABY0224	MAT**a** *ade2::ADE2*-P_{CLN2}-*CBP80NLS-rtTA(S2) ura3::URA3*-$P_{TETO2\text{-}CYC1}$-*lacZ*
ABY0243	MAT**a** *ade2::ADE2*-P_{CLB2}-*CBP80NLS-rtTA(S2) ura3::URA3*-$P_{TETO2\text{-}CYC1}$-*lacZ*
ABY0435	MAT**a** *ade2::ADE2*-P_{CLB2}-*rtT-GFP-A ura3::URA3*-$P_{TETO2\text{-}CYC1}$-*lacZ*
ABY0437	MAT**a** *ade2::ADE2*-P_{CLB2}-*rtT-GFP-A-SV40NLS ura3::URA3*-$P_{TETO2\text{-}CYC1}$-*lacZ*
ABY0439	MAT**a** *ade2::ADE2*-P_{CLB2}-*CBP80NLS-rtT-GFP-A ura3::URA3*-$P_{TETO2\text{-}CYC1}$-*lacZ*

Table S4. Primer sequences for RT-PRC: (5'-3')

Regions of *rtTA*, *lacZ* and *cdc28* mRNA were amplified by primers RTF+RTR, LAF+LAR, CDF+CDR respectitvely.

Primer name	Primer sequence
RTF	CGCGTACAGCCGCGCGCGTACGAAAAA
RTR	ATCGGTAAACATCTGCTCAAACTCGAA
LAF	GCTGGCGCAGGTAGCAGAGCGGGTAAA
LAR	ACGGGCTCCAGGAGTCGTCGCCACCAA
CDF	CGATAGTGAGATCGATCAGATTTTCAA
CDR	GGGTGGATGGCTGCTCTTCTGGCGCTAA

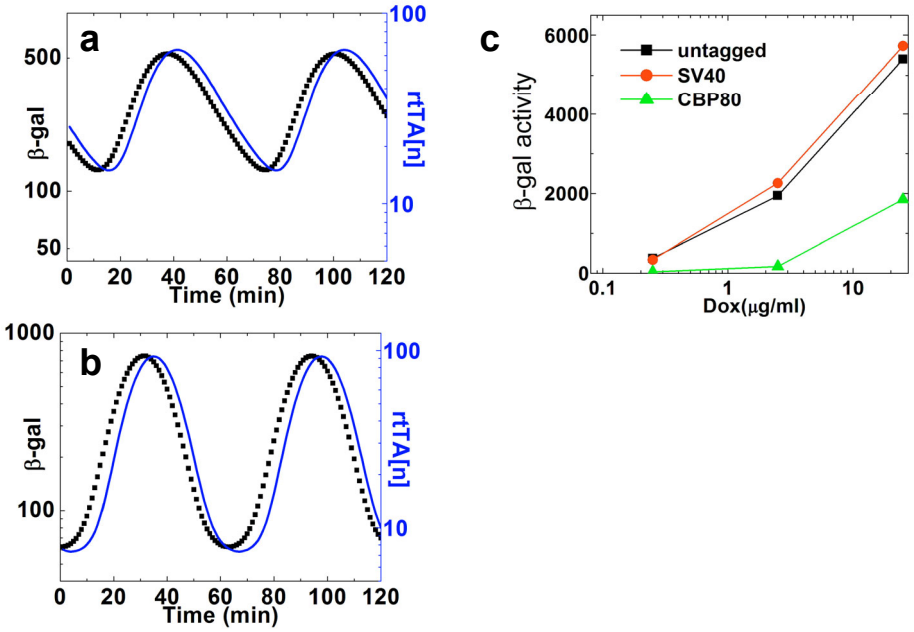

Figure S1. β-galactosidase activity, when *lacZ* is induced for short time intervals, reflects the nuclear concentration of rtTA. For numerical simulation, 15 minutes after addition of doxycycline transcription was allowed to proceed for 15 minutes so that lacZ mRNA was degraded at γ_L=0.04 min^{-1}. Functions and parameters for the input and nuclear rtTA correspond to that given in Fig 2c, d. The β-galactosidase activity is proportional to a 15 minutes integral value of *lacZ* mRNA level since β-galactosidase is a stable protein. The PTRs of the nuclear rtTA (blue lines) and the PTR of the 15 min integrals of corresponding β-gal activities (black squares) are very similar: 4.3 vs. 4.1 and 12.6 vs. 12, for slow (**a**) and fast (**b**) nuclear import rates, respectively. Changing γ_L in the relevant range of mRNA turnover does not significantly change the PTR of transiently expressed β-galactosidase activity. **c.** β-galactosidase activity, when *lacZ* is induced by untagged and NLS-tagged variants of rtTA driven by *CLN2* promoter at different doxycycline concentrations. Doxycycline at 0, 2.5 and 25 μg/ml concentrations was added for 2 hours. NLSs contain basic residues (Lys, Arg), while the VP16 domain in rtTA is an acidic domain (containing Glu). Therefore, the shorter classical NLS SV40 was attached to the C-terminal VP16 domain of rtTA, while the longer bipartite CBP80 NLS to the N-terminal DNA binding domain of rtTA (TetR), in order to avoid possible strong interference between VP16 and CBP80NLS. The rtTA and rtTA-SV40NLS display very similar induction curve, while CBP80NLS-rtTA — possibly due to a lower DNA binding affinity of the TetR domain — the induction curve is shifted towards higher doxycycline concentrations. The expression level of *lacZ* induced by CBP80NLS-rtTA at 25 μg/ml doxycycline concentration equals that of rtTA and rtTA-SV40NLS at 2.5 μg/ml.

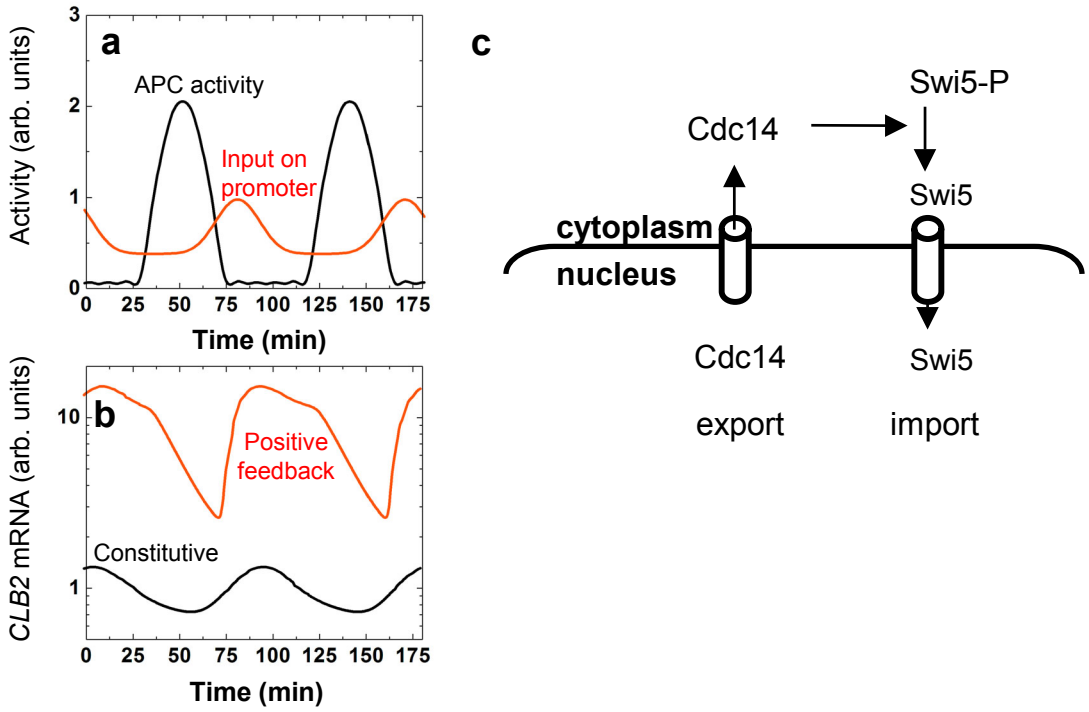

Figure S2. Input and output activities of the *CLB2* promoter with and without positive feedback. **a.** The low PTR oscillations in Fkh2 and Ndd1 activities determine the basal oscillations at P_{CLB2} (input on promoter, $f_{input}(t)$). Clb2 is periodically degraded by APC pathway in late mitosis and G1 phase (APC activity, $f_{APC}(t)$). **b.** *CLB2* mRNA expression. The following parameter values were taken: $\gamma = 0.053 min^{-1}$, $\kappa = 0.5\ min^{-1}$, n = 4, K = 2 (arbitrary units). The PTR for the expression with positive feedback (5.9) is more than three times higher than that for constitutive expression (PTR=1.8, without positive feedback).**c.** Coupled nuclear transport events in mitotic exit network. Nuclear Cdc14 phosphatase is released into the cytoplasm after a signal is propagated through the mitotic exit network involving several components. The cytoplasmic Cdc14 dephosphorylates Swi5, which in turn is imported into the nucleus.